ResearchGate

See discussions, stats, and author profiles for this publication at: https://www.researchgate.net/publication/252613191

A compact 3D imaging laser radar system using Geiger-mode APD arrays: System and measurements

Article *in* Proceedings of SPIE - The International Society for Optical Engineering · August 2003

DOI: 10.1117/12.501581

CITATIONS
54

READS
709

12 authors, including:

Richard M. Marino
Massachusetts Institute of Technology
24 PUBLICATIONS **669** CITATIONS

SEE PROFILE

Robert C Knowlton
University of Texas Medical School
143 PUBLICATIONS **5,589** CITATIONS

SEE PROFILE

Some of the authors of this publication are also working on these related projects:

Project Temporal lobe epilepsy neurophysiology View project

Project Equigen study of generic substitution View project

All content following this page was uploaded by Richard M. Marino on 28 July 2016.

The user has requested enhancement of the downloaded file.

A compact 3D imaging laser radar system using Geiger-mode APD arrays: system and measurements*

Richard M. Marino[1], Timothy Stephens, Robert E. Hatch, Joseph L. McLaughlin, James G. Mooney, Michael E. O'Brien, Gregory S. Rowe, Joseph S. Adams, Luke Skelly, Robert C. Knowlton, Stephen E. Forman, and W. Robert Davis

Massachusetts Institute of Technology, Lincoln Laboratory
244 Wood Street, Lexington, Massachusetts 02420-9108

ABSTRACT

MIT Lincoln Laboratory continues the development of novel high-resolution 3D imaging laser radar technology and sensor systems. The sensor system described in detail here uses a passively Q-switched solid-state frequency-doubled Nd:YAG laser to transmit short laser pulses (~ 700 ps FWHM) at 532 nm wavelength and derive the range to target surface element by measuring the time-of-flight for each pixel. The single photoelectron detection efficiency has been measured to be > 20 % using these Silicon Geiger-mode APDs at room temperature. The pulse out of the detector is used to stop a > 500 MHz digital clock integrated within the focal-plane array. With appropriate optics, the 32x32 array of digital time values represents a 3D spatial image frame of the scene. Successive image frames from the multi-kilohertz pulse repetition rate laser pulses are accumulated into range histograms to provide 3D volume and intensity information.

In this paper, we report on a prototype sensor system, which has recently been developed using new 32x32 arrays of Geiger-mode APDs with 0.35 μm CMOS digital timing circuits at each pixel. Here we describe the sensor system development and present recent measurements of laboratory test data and field imagery.

Keywords: Laser radar, ladar, 3D imaging, photon counting, avalanche photodiode array.

1. INTRODUCTION

MIT Lincoln Laboratory is developing laser and detector technologies that make it possible to build a three-dimensional laser radar (3D ladar) with several attractive features, including capture of an entire 3D image on a single laser pulse, tens of thousands of pixels, high frame rate, few-centimeter range resolution, and small size.[1-6] The laser technology is based on diode-pumped solid-state microchip lasers that are passively *Q*-switched.[5] The detector technology is based on arrays of avalanche photodiodes (APDs) operating in Geiger mode, with integrated timing circuitry for each pixel.[7-9]

Figure 1 shows the ladar concept. Light from the pulsed laser is diverged to illuminate the entire scene of interest. The reflected light is imaged onto a two-dimensional array of detectors. Rather than measuring intensity, these detectors measure the time of arrival of the reflected light. The time of arrival is linearly dependent on the range to the part of the scene imaged onto a detector. With each pixel coded with range, the ladar produces an angle-angle-range, or tri-dimensional, image from each laser pulse. As demonstrated by some of the 3D images shown herein, the ladar can be

* This research is sponsored by the Air Force under Contract F19628-00-C-0002. The views expressed are those of the authors and do not reflect the official policy or position of the U.S. government.

[1] marino@ll.mit.edu; phone 1 781 981-4011; fax 1 781 981-5069; ll.mit.edu

HESAI EX1028, P.2

Downloaded From: http://proceedings.spiedigitallibrary.org/ on 07/28/2016 Terms of Use: http://spiedigitallibrary.org/ss/TermsOfUse.aspx

used to penetrate foliage, and can provide images from perspectives other than that of the sensor. This ladar concept is well suited for robotic vision, navigation of autonomous vehicles, manufacturing quality control, industrial security, and topography.[10]

To further demonstrate the concept and utility for this type of 3D ladar, Lincoln Laboratory has constructed a third generation (Gen-III) ladar system using a 5 to 10-kHz microchip laser operating at 532 nm, a 32x32 array of Geiger-mode APDs integrated with >500 MHz CMOS timing circuitry, and the optics and mounting to allow the entire sensor to be scanned, building up images several thousand pixels in each angular direction. References 2–6 present details of the focal plane array technology and descriptions of the original Gen-I brassboard ladar. Along with examples of 3D imagery collected with it. In this paper, we show the integration of a ladar testbed based on the 32x32 generation of APD focal planes and present images gathered in the laboratory and in the field.

2. DESIGN AND PAREMETERS OF THE GEN-III LADAR SYSTEM

After the Gen-I ladar had proven the concept of using an array of APDs to capture high-resolution tri-dimensional (angle-angle-range) data, the next logical step was to increase the focal plane array size, reduce the size of the optical system and integrate a system with a much larger field of regard. The Gen-III system was conceived as a design study for the development of rugged and compact ladars with these enhanced characteristics, and has been constructed as such.

The design parameters for Gen-III are presented in Table 1 below. The optical design is illustrated in Figure 2. The transmit path starts with the microchip laser, whose operating wavelength was selected as 532 nm. The output beam passes through a beam-expanding telescope and then into a diffractive beam splitter, where it is split into a 32 by 32 array of beamlets to efficiently illuminate the individual fields of view of the 32 by 32 pixel APD array. The 1024 beamlets provide advantages over floodlit illumination including better geometric coupling, reduced background compared to micro lens coupled detectors, and increased angular resolution

Table 1. The optical design parameters of the Gen-III system.

Parameter	Specification
Laser Wavelength	532 nm
Receive aperture diameter	7.5 cm
Effective focal length	30.0 cm
Focal ratio	*f*/4.0
Number of pixels in FPA	32 x 32
Projected 100 µm pixel pitch	333 µrad
FOV (32 x 32)	10.3 mrad x 10.3 mrad
Range Resolution	15 cm
Transmitted far field pattern	32 x 32 spot array matched to detector arrays
Laser and Imaging rate	5000 to 10000 per s

After the beamsplitter, the 1024 beamlets pass through a focusing lens, a hole in the center of the transmit-receive beam splitter mirror, and collimating objective lens. The 32 by 32 array of beamlets is reflected from the target, returns through the objective lens, and is diverted to the APD array by the transmit-receive beamsplitter mirror.
One of the goals of the laser radar design is compact packaging. The transmit aperture has an 11-mm diameter, and the receive aperture has a 75-mm outer diameter and 17-mm inner diameter. The prime focal length is 300 mm. The

HESAI EX1028, P.3

Downloaded From: http://proceedings.spiedigitallibrary.org/ on 07/28/2016 Terms of Use: http://spiedigitallibrary.org/ss/TermsOfUse.aspx

transmit path length is 93 cm long, and the receive path length is 30 cm long. All optical component mounts are connected to a 165 x 170 x 6mm plate, which functions as an "optical bench". The optical bench and main structure is made of Invar because of its low coefficient of thermal expansion. Most of the transmitter components are located on one side of this plate, and the receiver components on the other. This arrangement was adopted to provide a compact common foundation for all of the elements, while allowing ready access for installation and adjustment. Both transmitter and receiver optical paths have multiple folds to reduce the required area of the bench. Both have been folded to fit in a 20-cm (< 8 liter) cube.

Figure 3 shows a three-dimensional view of the folded transmit and receive optical that supports these requirements. The monostatic architecture was chosen to provide a more compact design. The majority of transmit and receive optical elements are mounted on either sides of an internal optical bench. The focal plane and laser are relatively simple to remove and replace with other devices. A commercially available narrow bandpass filter (1 nm wide FWHM) was inserted to reduce background detections during daylight operations. The receive optics uses a single refractive element and brings the input light to an $f/4$ focus near the APD array.

Figure 4 presents a sketch of the integrated APD and CMOS timing circuit arrays along with photographs of the components and of the integrated package. The APD detector array is front-illuminated and uncoated. APDs have been fabricated with active areas of 30-µm and 40-µm diameters. The pixel pitch on the APD arrays is 100 µm, yielding 7% and 13% array fill factors. The diffractive optical element is used to create 32x32 spot array pattern at the target. The optics are aligned so that each laser spot is matched to an individual pixel IFOV. This has the effect of reducing background false detections and has the effect of increasing the fill factor of the detector array. CMOS timing circuitry integrated with 32x32 APD arrays provides the core range timing. The Lincoln Laboratory developed and fabricated APD/CMOS focal plane has the characteristics shown in Table 2.

Table 2. Geiger-mode APD/CMOS focal plane characteristics

Parameter	Measured Value
APD active area diameter	30 µm and 40 µm
Detection efficiency, η_{det}	> 20%
Pixel pitch	100 µm
CMOS clock rate	500 MHz
Operable Pixels	Greater than 99%

In order to function as a ladar system, an appropriate laser transmitter must be integrated into the system. Lincoln has designed and fabricated several such lasers, and the characteristics of the Gen-III transmitter are shown in Table 3. This laser uses a frequency-doubled and passively Q-Switched Nd:YAG laser. A separate photodiode is used to measure the transmit pulse and initiate the timing sequences of the system. With the detection and timing circuits operating as designed, the range resolution of the Gen-III system is limited by the pulse length and stability of the transmitter. Normal operation demonstrates a 700 ps (FWHM) pulse width and about 15 cm 1σ range resolution.

The Gen-III system was designed, fabricated, assembled and tested at Lincoln Laboratory. A significant portion of this effort was the development of the software that allows operator control of the test parameters (range, range gate, APD biases, etc.) and recording of the large amounts of data generated. At 10 kHz frame rate the raw data rate from the FPA readout card is 20 giga-Bytes per s. Figure 5 presents photographs of the integrated sensor head, and a rendition of the opto-mechanical design. The sensor head is 20 x 20 x 22 cm and weighs about 6 kg. As shown in Figure 6, the

HESAI EX1028, P.4

Downloaded From: http://proceedings.spiedigitallibrary.org/ on 07/28/2016 Terms of Use: http://spiedigitallibrary.org/ss/TermsOfUse.aspx

entire ladar sensor head was mounted on a commercial computer-controlled pan-tilt mount. With this setup, the ladar sensor was scanned to generate wider field of regard images.

Table 3. The laser transmitter characteristics

Parameter	Measured Value
Wavelength	532 nm
Pulse length	~ 700 psec
Energy per pulse	33 μJoules (at 532 nm)
Pulse repetition rate	5 to 10 kHz

3. GEN-III 3D-LADAR MEASUREMENTS

The first of the distances measured by counting clock pulses is the distance to the opening of the range gate. This is measured in quarter cycles of a master 125 MHz quartz crystal oscillator, and is set in meters from the operator's console. When the range gate is opened, the system counts quarter cycles of the ≈ 500 MHz CMOS clock to determine how far into the range gate the detection occurs. The detection itself shuts off the clock and the clock counts are recorded in the data stream. Because the CMOS clock rate is a function of temperature, its rate is automatically calibrated against the system clock every few seconds.

The high framing rate of these sensors affords the opportunity of detecting motions within the field of view. Figure 7 presents a few frames from a 10-second movie made of a automobile driving through the laser spot array at about 200 meters range. The framing rate for the sensor was 5000 Hz. Angle-angle-intensity images were derived from the probability of detection for each pixel over short time periods, like 30 ms for a 30 Hz movie sequence.

Because the Gen-III and similar systems rely upon the photon-counting ability of the Lincoln Geiger-mode APD/CMOS arrays, the sensitivity of these systems is extraordinary. The returned signal from the Gen-III sensor, measured in the number of detections or photoelectrons, N_{det}, is given by

$$N_{\mathrm{det}} = E_p \frac{\lambda}{hc} \tau_{to} \tau_{ro} \tau_{atm}^2 \frac{1}{N_{pix}} \rho_t \frac{A_{CA}}{\pi R^2} \eta_{\mathrm{det}} f_{tr} f_{ll}$$

where E_p is the laser pulse energy, R is the range to target, A_{CA} is the receiver clear aperture area, η_{det} is the detection efficiency, t_i is the transmission of the receive optics, transmit optics and atmosphere, f_{tr} is the fractional overlap of the transmit beam and receive FOV and f_{ll} is the efficiency of the optical coupling at the FPA.

4. THE GEN-III LADAR AND SOME SAMPLE IMAGES

The Gen-III ladar system was based on a 32x32 array of Geiger-mode APDs without microlenses and which transmitted a matrix of small spots at 532 nm. Figure 8 shows two visible photographs of a tank at a range of approximately 500 m. The upper image is a visible color photograph that was taken while the laser was off. The bottom photograph was set with a long exposure and green-enhanced to show an image of the 532 nm 32x32 laser spot pattern as it was backscattered from the target scene. Figure 9 shows a single perspective of the 3D point-cloud of data collected from a different tank vehicle also at 500 m range.

HESAI EX1028, P.5

Downloaded From: http://proceedings.spiedigitallibrary.org/ on 07/28/2016 Terms of Use: http://spiedigitallibrary.org/ss/TermsOfUse.aspx

The data shown in Figure 10 were also taken at the Eglin AFB ladar target test range and an example of a composite 3D imagery is presented here. This 3D image, which can again be rotated to provide viewing from any direction, covers an angular area of about 8 mr (one array width high) in elevation by about160 mr in azimuth. Multiple step-stare collections were combined to form this wide-angle image. 3D data detail of a tower base and a pair of resolution panels are shown as "zoomed-in" subsets of the composite image. This scanned imagery was assembled using the pan-tilt mount encoder readouts to position the individual images with respect to each other.

5. FOLIAGE PENETRATION EXPERIMENTS

The effective high-resolution imagery obtained with this photon-counting detection ladar led to the interest in imaging through foliage, where the goal was to visualize the 3D scene underneath. For these types of applications, the sensor actually works better with a relatively low probability of detecting the in-range obscurant or foliage. This can be arranged in any of several ways including reducing the laser power or apodizing the receive aperture with an iris or electronically reducing the sensitivity of the detector. The sensor can then be used to measure a 3D histogram of detections under the obscurant or foliage. In order to investigate this capability, the Gen-III system was placed on an elevator of the 300 ft tower at the Russell Measurement Facility Tower at Redstone Arsenal, in Huntsville, AL.

The sensor was arranged to have a clear line of sight to the foliated ground area near the base of the tower. Once the data are collected, they can be manipulated as a 3D cloud of points. Figure 11 shows photographs of the scene from above and from the ground level. Objects located under the trees include three wooden picnic tables, a wooden gazebo, a HUMVEE military vehicle, and two rental cars (the ground-level photo was taken when only one rental car was present). Figure 12 shows an example of a single 3D image data set that was recorded from the top floor of the tower. The sequence of images shows how compressing the color bar of the display can expose the 3D scene structure on the ground. The shadow from the in-range trees and foliage appears as black patches or holes within the scene. This example shows that even from a single sensor viewing direction, the size and shape of the objects under trees can be measured with the ladar 3D spatial data. We are investigating algorithms to accumulate the 3D data from a variety of sensor viewing directions with the motivation of filling-in some of the volumes that are shadowed or heavily obscured from any single viewing direction.

6. FUTURE DEVELOPMENT OF 3D LADAR

Demonstrations of 32x32 focal-plane arrays of integrated Geiger-mode APDs and CMOS timing circuitry have now been made and will continue. Two such devices have been incorporated into 3D-ladar systems that have been demonstrated in field tests. Scaling up the focal-plane array to more elements, such as 128x128, will be relatively straightforward, since microelectronics techniques are used. Because the current Geiger-mode APDs are made of silicon and do not respond well to wavelengths beyond about 900 nm, we are developing Geiger-mode APD arrays with III-V materials that respond to longer wavelengths, such as those in the eye-safe regime around 1500 nm.

The energy per pulse (up to about 33 μJ at 532 nm) and repetition rate (up to about 10,000 Hz) from existing microchip lasers are sufficient for many applications. For applications requiring more laser pulse energy, it is possible to couple a microchip laser to a diode-pumped solid-state amplifier. Operation of a 3D laser radar at eye-safe wavelengths (~ 1500 nm) can be achieved by using microchip lasers to pump optical parametric oscillators.[11]

With microchip lasers and microelectronic arrays of detectors and timing circuitry, we expect that an entire 3D ladar can be fit into a package small enough (the size of a coffee can) and light enough (less than one kilogram) to be handheld. These 3D ladars will be able to record a 3D image with thousands of pixels on a single laser pulse and have many-kilohertz frame rates. Hundreds of frames could be processed in a fraction of a second in order to see through obscurants, to freeze motion in a dynamic scene or in the ladar platform, or to extend the effective range.

HESAI EX1028, P.6

Downloaded From: http://proceedings.spiedigitallibrary.org/ on 07/28/2016 Terms of Use: http://spiedigitallibrary.org/ss/TermsOfUse.aspx

7. ACKNOWLEDGEMENTS

We would like acknowledge and give thanks to Ray Balcerak and DARPA for supporting this research and providing the challenge; to Dr. Brian F. Aull and his team at Lincoln Laboratory for developing this remarkable FPA technology; to Dr. Brian H. Miles and his crew for supporting the tests at Eglin AFB, and to Mr. J. Eddie Batt of the U.S. Army AMCOM MRDEC and his crew for supporting the tests at the Russell Measurement Facility.

REFERENCES

1. R.M.Marino, R.M.Spitzberg, M.J.Bohrer, "A Photon Counting 3-D Imaging Laser Radar for Advanced Discriminating Interceptors*;"* 2nd Annual AIAA SDIO Interceptor Technology Conference, AIAA 93-2669, Albuquerque, NM, June 1993
2. R.M.Marino, M.J.Bohrer; "A Photon-Counting 3-D Imaging Laser Radar*," Lasers '94*, Quebec City, Quebec, December 1994.
3. R.M. Heinrichs, B.F. Aull, R.M. Marino, D.G. Fouche, A.K. McIntosh, J.J. Zayhowski, T. Stephens, M.E. O'Brien, M.A. Albota, "Three-Dimensional Laser Radar with APD Arrays*,"* Proc. SPIE Laser Radar Technology and Applications VI, Vol. 4377, April 2001
4. M.A. Albota, B.F. Aull, D.G. Fouche, R.M. Heinrichs, D.G. Kocher, R.M. Marino, J. Mooney, N.R. Newbury, M. O'Brien, B.E. Player, B.C. Willard, J.J. Zayhowski, "Three-Dimensional Imaging Laser Radar with Geiger-mode Avalanche Photodiode Arrays*,"* MIT Lincoln Journal, Vol. 13, No. 2, 2002
5. B.F. Aull, A.H. Loomis, D.J. Young, R.M. Heinrichs, B.J. Felton, P.J. Daniels, and D.J. Landers, "Geiger-mode Avalanche Photodiodes for Three-Dimensional Imaging," Linc. Lab. J. Vol. 13, No. 2, 2002.
6. M.A. Albota, R.M. Heinrichs, B.F. Aull, R.M. Marino, D.G. Kocher, D.G. Fouche, J.J. Zayhowski, B.E. Player, B.C. Willard, J. Mooney, M.E. O'Brien, and R.R. Carlson, "Three-Dimensional imaging laser radar with a photon-counting avalanche photodiode array and microchip laser*,* Applied Optics," Vol. 41, No. 36, December 2002
7. J.J. Zayhowski and C. Dill III, "Diode-Pumped Passively Q-Switched Picosecond Microchip Lasers," Opt. Lett*.* 9 (18),1994, pp. 1427–1429.
8. J.J. Zayhowski, "Passively Q-Switched Microchip Lasers and Applications," *Rev. Laser En*g. 29 (12), 1988, pp. 841–846.
9. J.J. Zayhowski, C. Dill III, C. Cook, and J.L. Daneu, "Mid-and High-Power Passively Q-Switched Microchip Lasers," *OSA TOPS* 26, *Advanced Solid-State Laser*s, *Topical Mtg., 31 Jan.–3 Feb. 1999,* pp. 178–186.
10. R.M. Marino, "Method and Apparatus for Imaging a Scene Using a Light Detector Operating in Non-linear Geiger-mode," U.S. Patent No. 5,892,575 (6 April 1999).
11. J.J. Zayhowski, "Periodically poled lithium niobate optical parametric amplifiers pumped by high-power passively Q-switched microchip lasers," *Opt. Lett.* **22**, 169–171, 1 Feb 1997.

HESAI EX1028, P.7

Downloaded From: http://proceedings.spiedigitallibrary.org/ on 07/28/2016 Terms of Use: http://spiedigitallibrary.org/ss/TermsOfUse.aspx

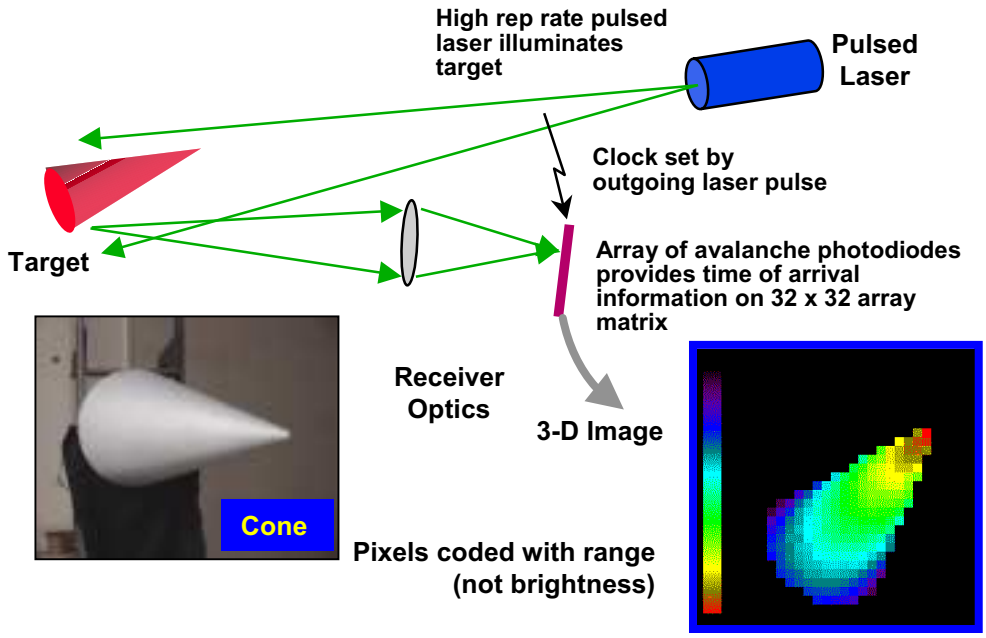

Figure 1: Basic concept for tri-dimensional (angle-angle-range) laser radar. The entire scene is flood illuminated and imaged on each laser pulse.

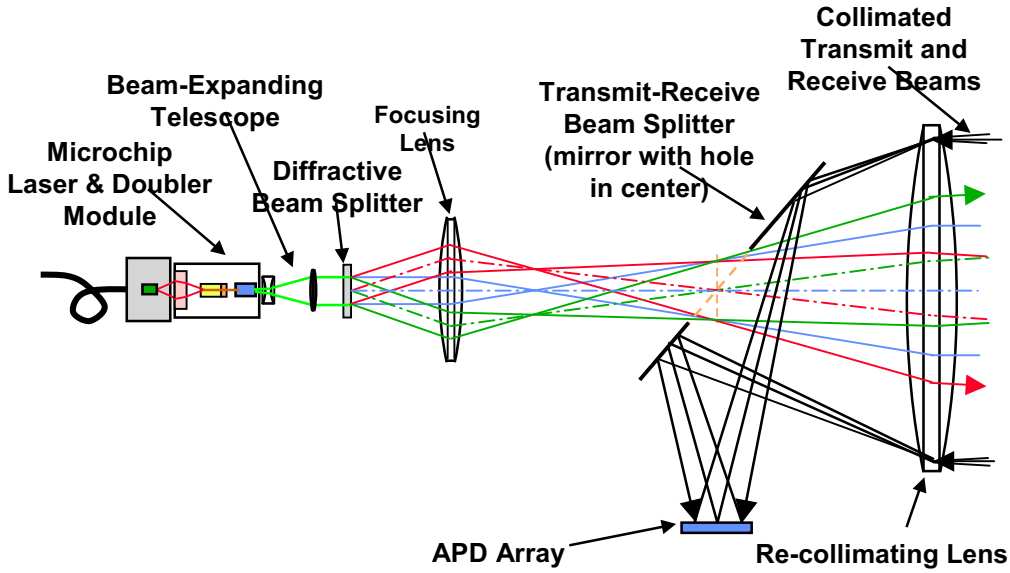

Figure 2: The Gen-III sensor optical design.

HESAI EX1028, P.8

Downloaded From: http://proceedings.spiedigitallibrary.org/ on 07/28/2016 Terms of Use: http://spiedigitallibrary.org/ss/TermsOfUse.aspx

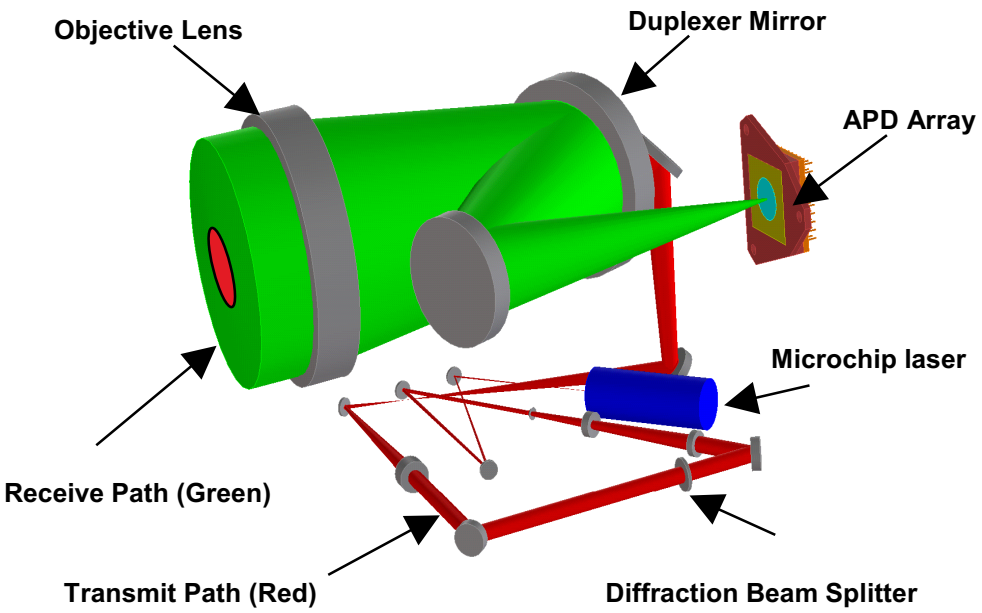

Figure 3: A CAD model of the Gen-III sensor optical design. The transmit portion is shown in red while the receive path is shown in green.

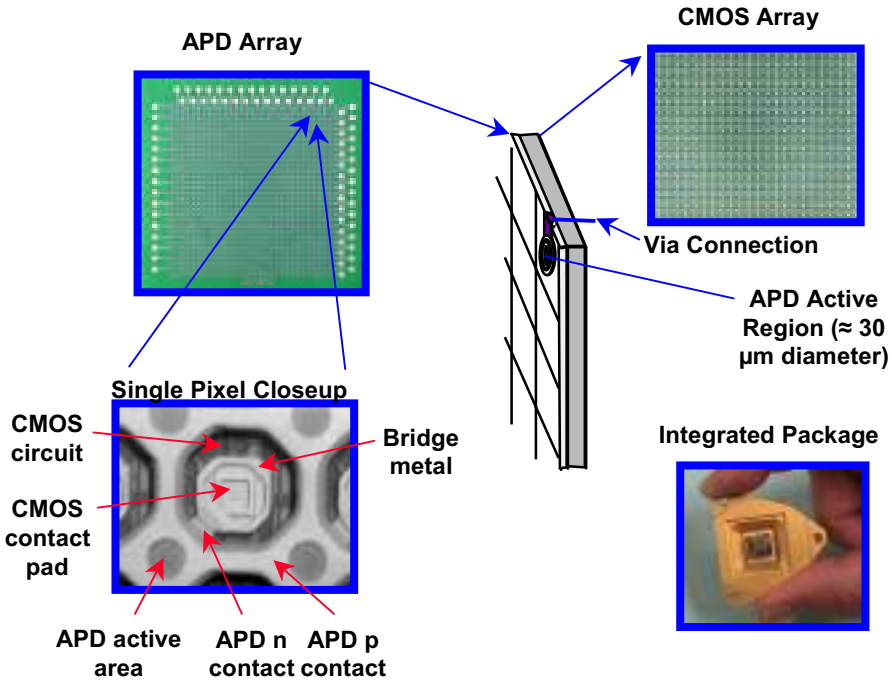

Figure 4: The Lincoln fabricated and assembled 32x32 APD/CMOS focal plane array. The microlens array can be used to image the exit pupil of the receive optics onto the APD active area, but was not used in the Gen-III system.

HESAI EX1028, P.9

Downloaded From: http://proceedings.spiedigitallibrary.org/ on 07/28/2016 Terms of Use: http://spiedigitallibrary.org/ss/TermsOfUse.aspx

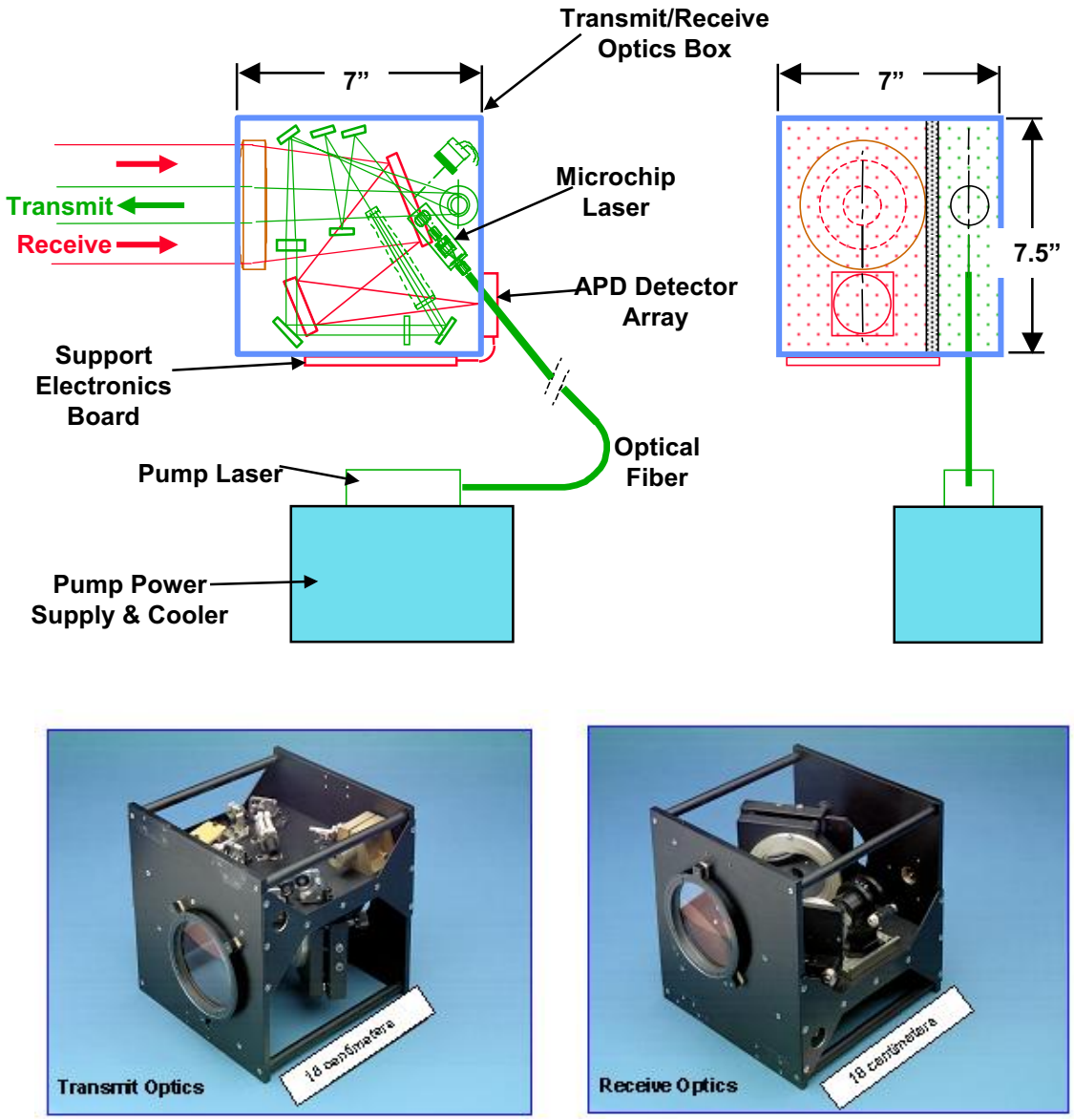

Figure 5: The optical system of the Gen-III Ladar testbed. The monostatic architecture was chosen to provide a compact design. The majority of the transmit and receive optics are on either sides of an internal optical bench. The focal plane and laser are relatively simple to remove and replace with other devices. Photographs of the sensor optical head are shown at the bottom.

HESAI EX1028, P.10

Downloaded From: http://proceedings.spiedigitallibrary.org/ on 07/28/2016 Terms of Use: http://spiedigitallibrary.org/ss/TermsOfUse.aspx

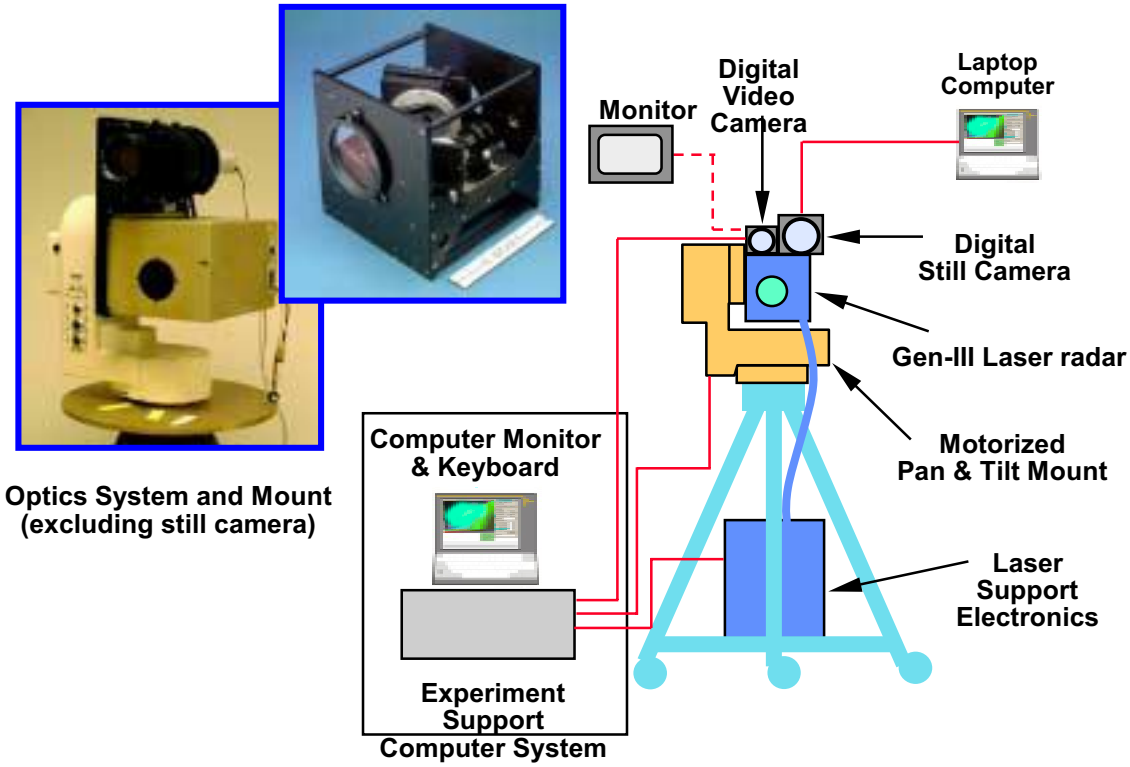

Figure 6: Experimental set-up for the Gen-III system showing the major components. The sensor system was integrated onto a computer-controlled pan-tilt mount for data acquisition in the field.

HESAI EX1028, P.11

Downloaded From: http://proceedings.spiedigitallibrary.org/ on 07/28/2016 Terms of Use: http://spiedigitallibrary.org/ss/TermsOfUse.aspx

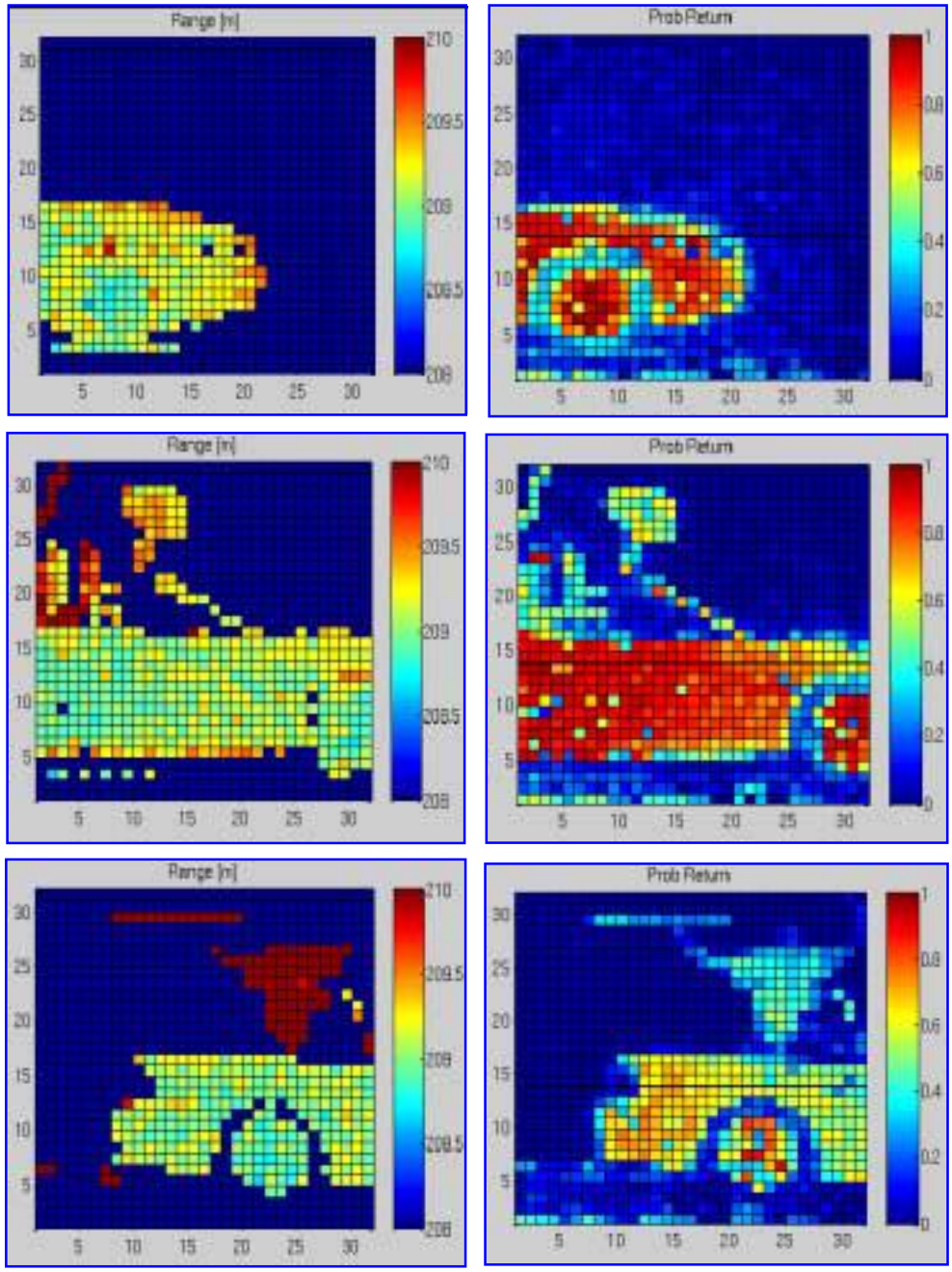

Figure 7: Three 32x32 3D image frames from a 10-second movie made at a range of 209 meters with the Gen-III system. The automobile was driven through the laser beam spot pattern. On the left, the color coding indicates range within the 2-meter range window. On the right the color represents probability of detection.

HESAI EX1028, P.12

Downloaded From: http://proceedings.spiedigitallibrary.org/ on 07/28/2016 Terms of Use: http://spiedigitallibrary.org/ss/TermsOfUse.aspx

Figure 8: Two photographs of a tank vehicle. The upper image is a visible color photograph that was taken while the laser was off. The bottom photograph was set with a long exposure and green-enhanced to show an image of the 532 nm 32x32 laser spot pattern as it was backscattered from the target scene.

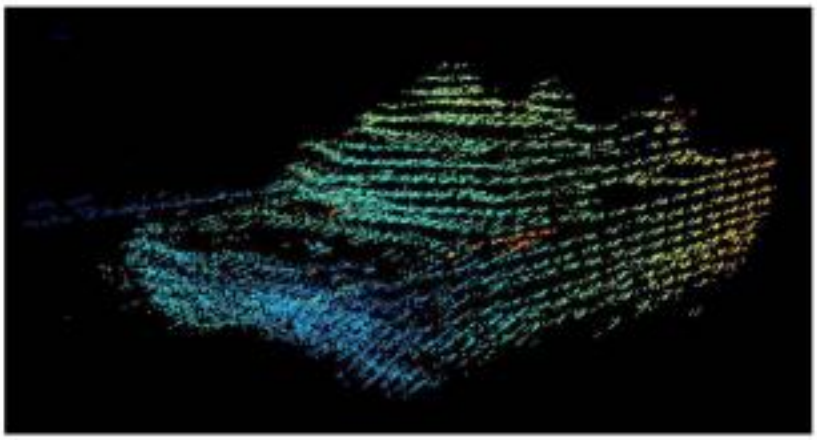

Figure 9: An example of a 3D image of a tank at a range of 500 m. Although the measurements were taken from one perspective, one the data are collected, they can be manipulated in the display and shown from any viewing direction.

HESAI EX1028, P.13

Downloaded From: http://proceedings.spiedigitallibrary.org/ on 07/28/2016 Terms of Use: http://spiedigitallibrary.org/ss/TermsOfUse.aspx

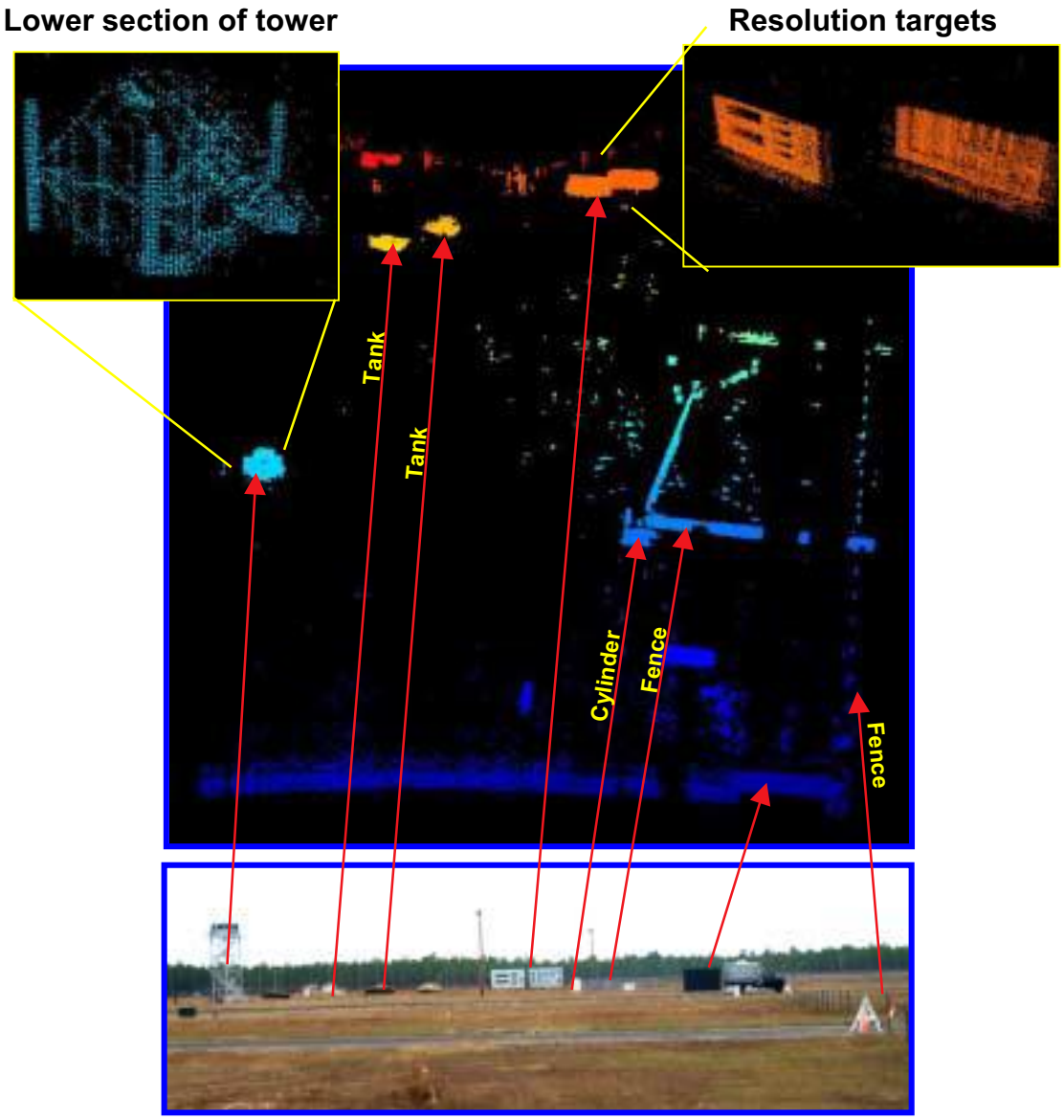

Figure 10: Tri-dimensional imagery of the Eglin AFB test range taken with the Gen-III system. This imagery may be rotated to be viewed from any direction. The reader is reminded that these data were taken from a single, stationary vantage point. The photograph was taken from the same position as the tri-dimensional imagery. The truck in the right foreground was moved prior to the Gen-III tests.

HESAI EX1028, P.14

Downloaded From: http://proceedings.spiedigitallibrary.org/ on 07/28/2016 Terms of Use: http://spiedigitallibrary.org/ss/TermsOfUse.aspx

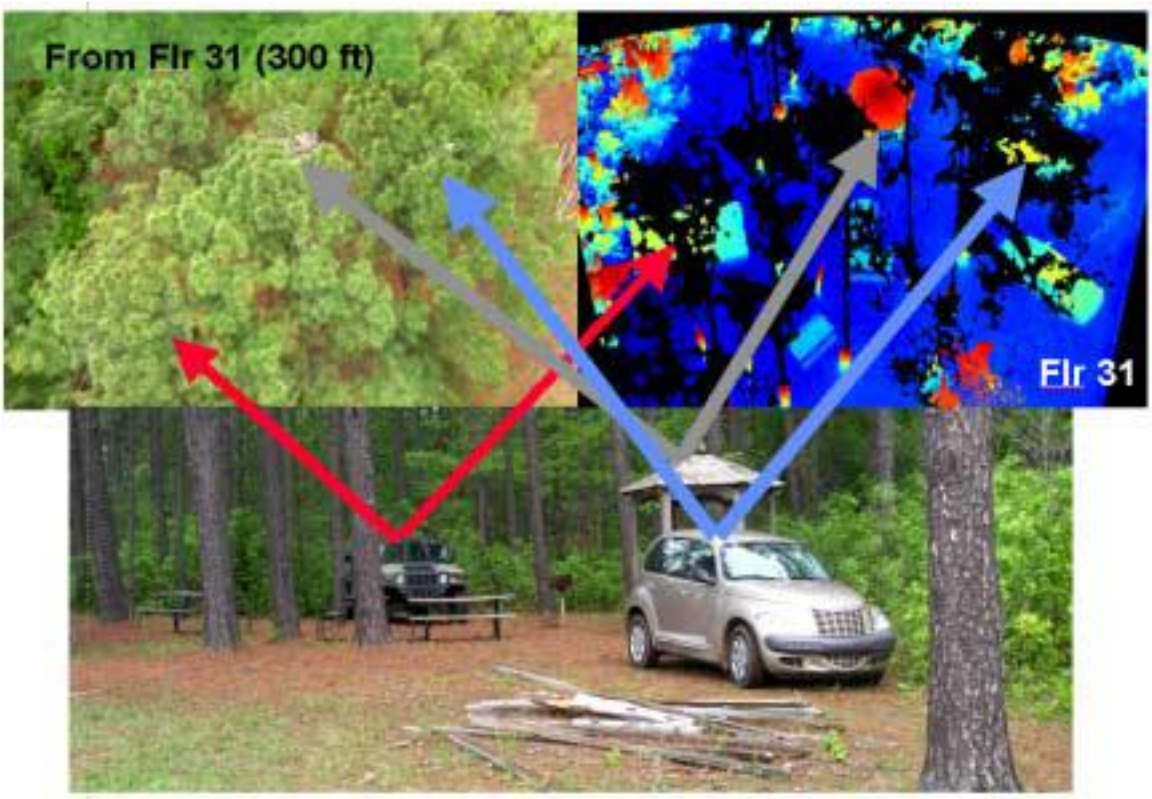

Figure 11: Photographs of the scene and a tree-cropped 3D image with several under-tree objects pointed out. The upper-left photograph was taken from the 31st floor (300 ft above the ground). The photograph in the bottom shows the objects under trees from the ground level. The color in the 3D image represents the calculated height above the ground plane. The data from the in-range foliage have been "cropped-off" by adjusting the color bar mapping. A wooden gazebo, three wooden picnic tables, a HUMVEE and two rental cars were in the scene during the measurements.

Downloaded From: http://proceedings.spiedigitallibrary.org/ on 07/28/2016 Terms of Use: http://spiedigitallibrary.org/ss/TermsOfUse.aspx

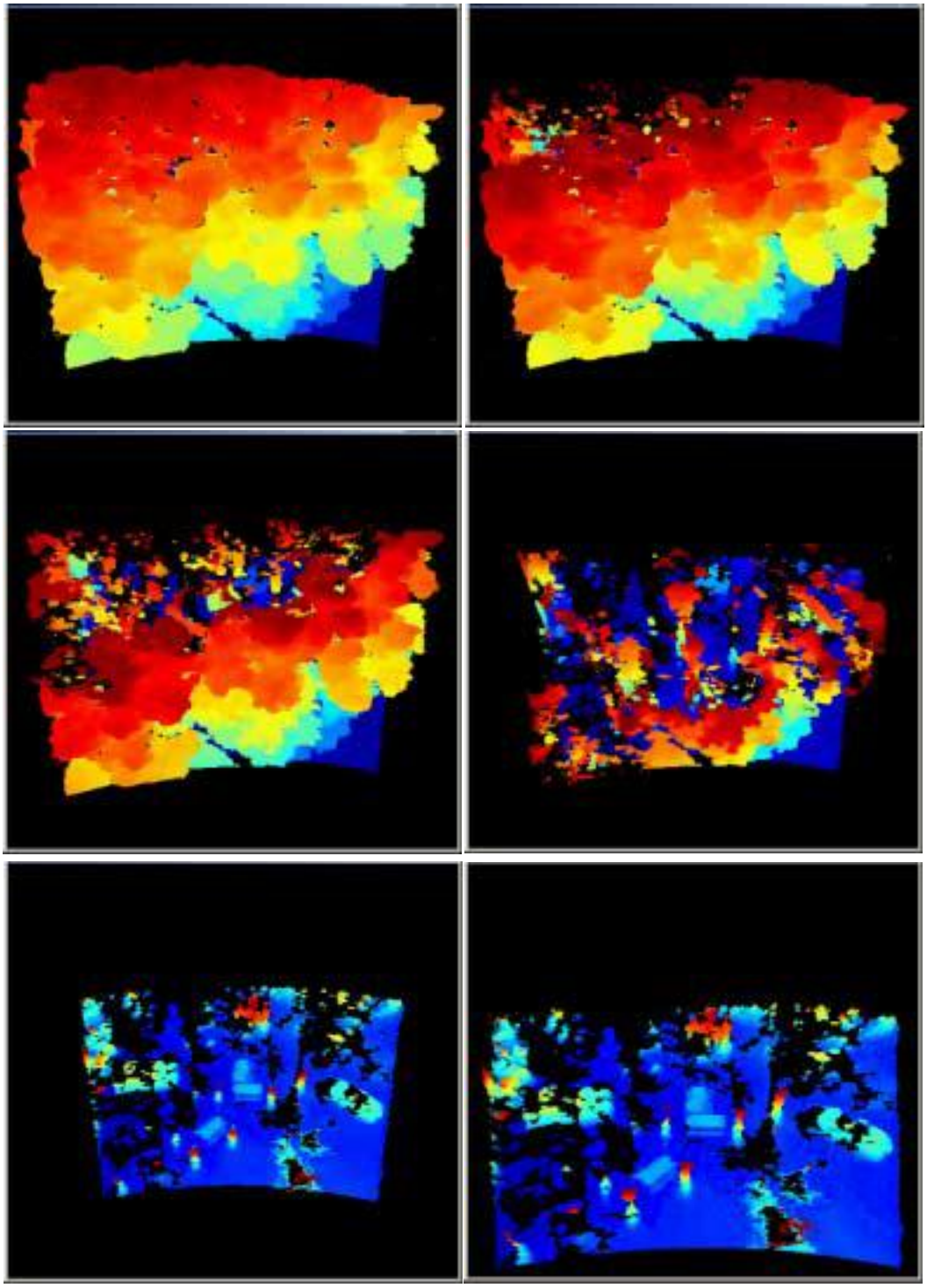

Figure 12: An example of a single 3D image point-cloud. From upper left to lower right, the color band was compressed to effectively crop-off the foliage above the scene on the ground.

HESAI EX1028, P.16

Downloaded From: http://proceedings.spiedigitallibrary.org/ on 07/28/2016 Terms of Use: http://spiedigitallibrary.org/ss/TermsOfUse.aspx